

Nonlinear optical susceptibilities of conjugated polymers: Damping, resonances, and scaling laws

V. A. Shakin*

Department of Physics, University of Tokyo, 7-3-1 Hongo, Bunkyo-ku, Tokyo 113, Japan

S. Abe

Electrotechnical Laboratory (ETL), 1-1-4 Umezono, Tsukuba 305, Japan

*and Joint Research Center for Atom Technology (JRCAT), National Institute for Advanced Interdisciplinary Research (NAIR),
1-1-4 Higashi, Tsukuba 305, Japan*

T. Kobayashi

Department of Physics, University of Tokyo, 7-3-1 Hongo, Bunkyo-ku, Tokyo 113, Japan

(Received 5 July 1995; revised manuscript received 24 October 1995)

Third-order nonlinear optical spectra $\chi^{(3)}$ of conjugated polymers are theoretically studied within the treatment of double-excitation configuration interaction for the Pariser-Parr-Pople model. We consider a realistic situation of dephasing rates being much larger than depopulation rates. It is shown that, on the low-energy side of the one-photon resonance, the absolute value of $\chi^{(3)}(-\omega; \omega, -\omega, \omega)$ is approximately proportional to the linear absorption spectrum $\alpha(\omega)$. Additional peaks show up in the $\chi^{(3)}$ spectrum at frequencies corresponding to energy differences among excited states. Their intensities can become comparable to and even stronger than ordinary two-photon absorption peaks in the same energy region. The same is true for the electromodulation spectrum $\chi^{(3)}(-\omega; \omega, 0, 0)$. In this situation the product of $\chi^{(3)}(-\omega; \omega, 0, 0)$ and $\alpha(\omega)$ is shown to be approximately proportional to $\chi^{(3)}(-\omega; \omega, -\omega, \omega)$.

I. INTRODUCTION

Conjugated polymers accommodate delocalized π electrons, which are responsible for many interesting electronic and optical properties. The relatively large optical nonlinearity of this class of materials makes it possible to obtain information about the nature of electronic excited states through various nonlinear spectroscopic measurements such as degenerate four-wave mixing, two-photon absorption, electroabsorption, and third harmonic generation.¹⁻⁵ Important issues discussed in the past included the energy locations and symmetries of low-lying excited states,³ the excitonic nature of one-photon excited states,⁴⁻⁸ and the role of biexcitons in two-photon resonances.⁹⁻¹¹

In a previous paper¹⁰ two of the present authors calculated $\chi^{(3)}(-\omega; \omega, -\omega, \omega)$ of conjugated polymers by use of the double-excitation configuration-interaction method for the Pariser-Parr-Pople model to find the electronic excited states, focusing on the biexciton-related two-photon absorption peaks located below the exciton resonance energy. We used the Orr-Ward formula¹² for $\chi^{(3)}$, in which damping was incorporated by adding imaginary parts to the energies of excited states. Although this approach was suitable for a discussion of two-photon excited states, there is a certain limitation in its applicability: it cannot be used for the important frequency region of the one-photon resonance, and also it neglects contributions of dephasing induced extra resonances.^{13,14} In order to deal with these effects, in the present paper we employ an alternative expression of $\chi^{(3)}$ derived from the Liouville equation of motion for the density matrix.¹³ We discuss the role of longitudinal and transverse relaxation rates in $\chi^{(3)}(-\omega; \omega, -\omega, \omega)$ as well as in the elec-

tromodulation spectrum $\chi^{(3)}(-\omega; \omega, 0, 0)$. We will demonstrate that, when the transverse relaxation (or dephasing) rate is much larger than the longitudinal relaxation (or depopulation) rate as in a usual situation, the contributions of extra resonances can become comparable to or even stronger than those of two-photon resonances. This implies that one has to be very careful in interpreting experimental data.

Another issue we discuss in the present paper is the relationship between the magnitude of $\chi^{(3)}(-\omega; \omega, -\omega, \omega)$ and the linear absorption spectrum $\alpha(\omega) = \text{Im}[\chi^{(1)}(\omega)]$ around the one-photon resonance peak. Bubeck *et al.*¹⁵ analyzed their degenerate four-wave mixing data for various materials and various frequencies, and proposed scaling laws between $\chi^{(3)}$ and α : in the case of conjugated polymers, $\chi^{(3)}(-\omega; \omega, -\omega, \omega)$ is almost proportional to $\alpha(\omega)$. They interpreted this result on the basis of the phase-space filling model and the assumption of large inhomogeneous broadening. We will demonstrate here that the linear relationship between $\chi^{(3)}(-\omega; \omega, -\omega, \omega)$ and $\alpha(\omega)$ approximately holds even for a single chain of polymer without inhomogeneous broadening, if the transverse relaxation rate is much larger than the longitudinal one.

II. THEORETICAL APPROACHES FOR $\chi^{(3)}$

There are two main approaches to derive an expression for $\chi^{(3)}$ on the microscopic basis. The first one utilizes the time-dependent perturbation theory to find a solution of the Schrödinger equation, which is supposed to be suitable to describe the behavior of the quantum system under consideration. The formula obtained in this way is usually called the Orr-Ward formula.¹² Clearly, the use of a wave function to describe the system does not allow us to take rigorously into account the process of the radiation absorption, because the latter necessarily involves an interaction of the system

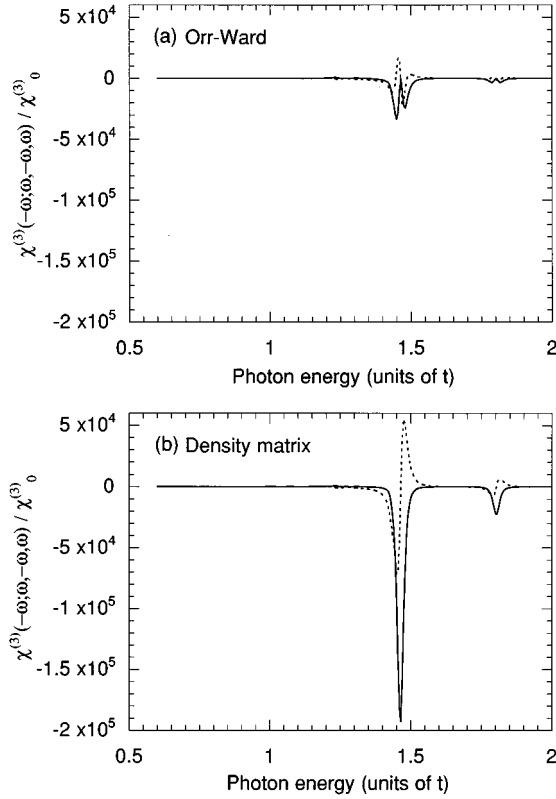


FIG. 1. The real (dashed line) and imaginary (solid line) parts of $\chi^{(3)}(-\omega;\omega,-\omega,\omega)$ as functions of photon energy for the polymer ring of $N=30$ sites with $\delta t=0.1t$. Through the whole paper the electron-electron potential used is the Pople potential with $U=2t$ and $V=t$. (a) is calculated using the Orr-Ward formula with $\hbar\Gamma=0.02t$, and (b) is obtained in the density-matrix formalism with $\hbar\Gamma_1=\hbar\Gamma_2=0.02t$.

with a reservoir. The absorption can be included here by simply allowing the energies of the system to be complex numbers. The Orr-Ward formula for $\chi^{(3)}$ is relatively compact, valid for the treatment of two-photon resonances,¹² and easy to compute. That was the reason why we used it in Ref. 10 to calculate two-photon absorption spectra.

The Orr-Ward approach treats only the resonances that do not produce a significant excited-state population.¹² That is why the Orr-Ward formula is not applicable, for example, in such an important frequency region as the region of absorption saturation. Also, we should not expect it to give correct results if the photon energy is close to other resonant transitions involving long-living one-photon excited states. To analyze such cases we can use another approach, namely the density-matrix formalism, which correctly allows for interaction with a reservoir. A general scheme to calculate nonlinear susceptibilities is based on a perturbation expansion of the density matrix of the quantum system.¹⁶ The damping relaxation is supposed to be governed by the following equations for the off-diagonal and diagonal density-matrix elements:

$$\left(\frac{\partial \rho_{nm}}{\partial t}\right)_{\text{damping}} = -\Gamma_{nm} \rho_{nm} \quad (n \neq m), \quad (1)$$

$$\left(\frac{\partial \rho_{nn}}{\partial t}\right)_{\text{damping}} = -\Gamma_{nn} (\rho_{nn} - \rho_{nn}^0), \quad (2)$$

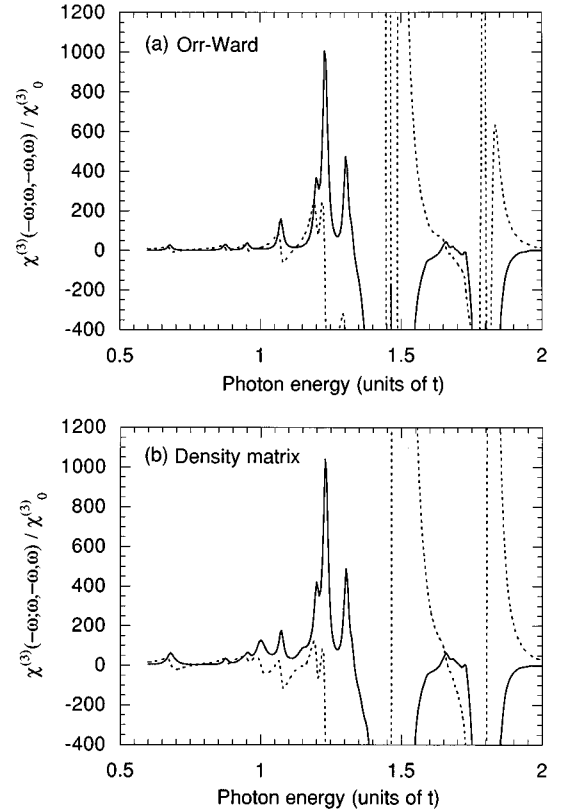


FIG. 2. The resolved two-photon absorption region of the spectra presented in Fig. 1.

where Γ_{nm} ($n \neq m$) and Γ_{nn} are the transverse and longitudinal damping constants, respectively. Inverse values of the damping constants are called the transverse and longitudinal relaxation times, respectively. It should be noted that, in general, in a multilevel system with all levels participating in the relaxation of the excess population in the given n th level, Eq. (2) is not correct, but can be considered a good approximation in the case for optically excited states.¹⁷

A completely general expression for $\chi^{(3)}(-\omega_1, -\omega_2 - \omega_3; \omega_1, \omega_2, \omega_3)$ can be found, for example, in Ref. 18. In this work we are interested specifically in $\chi^{(3)}(-\omega; \omega, -\omega, \omega)$ and $\chi^{(3)}(-\omega; \omega, 0, 0)$ spectra, expressions of which can be found from the general one choosing properly the values of ω_1 , ω_2 , and ω_3 . The former susceptibility is responsible for such important nonlinear processes as degenerate four-wave mixing, two-photon absorption, and absorption saturation. The latter determines the change of optical constants such as refractive index and absorptivity under an applied static electric field. A complete expression for $\chi^{(3)}(-\omega; \omega, -\omega, \omega)$ can be found, for example, in Ref. 19, and we present it in Appendix A (blocks are labeled in accordance with the corresponding terms in Ref. 18) for the case of zero temperature. Here we deal with a polymer ring, so that we consider only the case of all the relevant dipole operator components parallel to some specified axis. An expression for $\chi^{(3)}(-\omega; \omega, 0, 0)$ is given in Appendix B. Unlike the Orr-Ward formula, the triple summation here cannot be reduced to the product of ordinary series, therefore the numerical computation time is drastically increased. This is the reason why here we consider polymer rings with smaller number of sites than in Ref. 10.

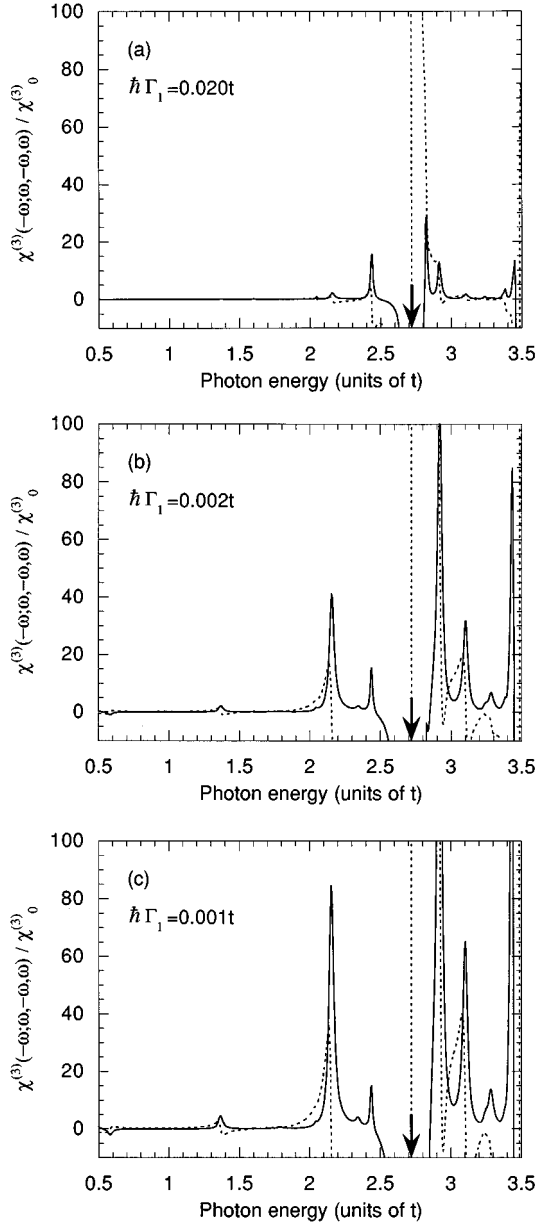


FIG. 3. The real (dashed line) and imaginary (solid line) parts of $\chi^{(3)}(-\omega; \omega, -\omega, \omega)$ as functions of photon energy for the polymer ring of $N=6$ sites with $\delta t=0.2t$, and $\hbar\Gamma_2=0.020t$. The vertical arrow points the lowest one-photon resonance. (a) $\hbar\Gamma_1=0.020t$. (b) $\hbar\Gamma_1=0.002t$. (c) $\hbar\Gamma_1=0.001t$.

III. TWO-PHOTON ABSORPTION AND SCALING RELATIONSHIP

Certainly it is interesting to compare results obtained with the Orr-Ward formula¹⁰ and in the density-matrix formalism. However, in doing so one must be aware of the qualitative difference between these two approaches, because in introducing the damping in the Orr-Ward scheme it is, for example, impossible to make a distinction between the longitudinal and transverse dampings. To avoid such a problem we take the same values for all damping constants in both approaches. Figures 1 and 2 show $\chi^{(3)}(-\omega; \omega, -\omega, \omega)$ per site of a polymer ring with $N=30$ sites. Here we use the same designations for parameters of the polymer chain and the

TABLE I. Excitation energies (in units of t) of one- and two-photon excited states for the polymer ring of $N=6$ sites with $\delta t=0.2t$. Electron-electron interaction is modeled by the Pople potential with on- and off-site Coulomb potentials $U=2t$ and $V=t$, respectively. A transition between the one-photon-excited level of $2.721t$ and the two-photon excited level of $4.876t$ contributes to the resonance peak in Fig. 3 at $\hbar\omega=2.155t$.

Number	One-photon excited states		Two-photon excited states	
	Energy	Energy	Energy	Half-energy
1	2.721	2.140	1.070	
2	3.481	3.202	1.601	
3	4.848	4.088	2.044	
4	5.864	4.447	2.223	
5	6.039	4.509	2.255	
6	6.344	4.876	2.438	
7	6.975	5.337	2.669	
8	9.277	5.457	2.729	
9		5.645	2.822	
10		5.825	2.912	
11		6.341	3.170	
12		6.471	3.236	
13		6.729	3.365	
14		6.764	3.382	
15		6.913	3.456	
16		7.564	3.782	
17		7.780	3.890	
18		8.481	4.240	
19		9.728	4.864	

same procedure for eigenstates calculation as in Ref. 10: t is an averaged magnitude of the transfer integral, δt is its modulation, U and V are the on- and off-site Coulomb potentials of the electron-electron interaction (all the data presented here were calculated using the Pople potential with $U=2t$ and $V=t$), Γ is the broadening constant in the Orr-Ward formula, and Γ_1 and Γ_2 are the longitudinal and transverse damping constants, respectively, in the density-matrix formalism. Normalization constants $\chi_0^{(1)}$ and $\chi_0^{(3)}$ are defined as

$$\begin{aligned}\chi_0^{(1)} &= e^2 a^2 / t, \\ \chi_0^{(3)} &= e^4 a^4 / t^3,\end{aligned}\tag{3}$$

where e is the electron charge and a is the averaged distance between adjacent sites. Figure 1 clearly demonstrates the failure of the Orr-Ward formula to describe the region of the saturation absorption. In the two-photon absorption region, which is resolved in Fig. 2, the difference is tiny, and the spectrum obtained in the density-matrix formalism demonstrates only some additional peaks, which are the result of the additional resonances corresponding to the energy difference between one- and two-photon excited states (see below).

However, such good agreement fails to be satisfied if we drastically decrease the ratio of Γ_1 to Γ_2 . To demonstrate this we show in Fig. 3 the spectra of $\chi^{(3)}(-\omega; \omega, -\omega, \omega)$ calculated using the density-matrix formalism for a relatively small ($N=6$) polymer ring (to avoid a complexity in the assignment

of resonant peaks). Excitation energies of the one- and two-photon excited states are presented in Table I. Figure 3(a) is for $\hbar\Gamma_1 = \hbar\Gamma_2 = 0.020t$, while Figs. 3(b) and 3(c) are for $\hbar\Gamma_1 = 0.002t$ and $0.001t$, respectively, keeping $\hbar\Gamma_2 = 0.020t$. The vertical arrow points out the lowest one-photon resonance (at $\hbar\omega = 2.721t$). In Fig. 3(a) the largest peak in the region below the one-photon resonance (at $\hbar\omega = 2.438t$) corresponds to the two-photon excited state with an excitation energy of $4.876t$, but the doubled photon energy of another resonance peak lying $0.3t$ lower (at $\hbar\omega = 2.155t$) does not match with any two-photon excited state. This resonance energy equals the energy difference between the one-photon ($2.721t$) and two-photon ($4.876t$) excited states, and the corresponding resonance comes from blocks (b_1) , (a_2) , (c_2) and (d_1) in the expression of $\chi^{(3)}(-\omega; \omega, -\omega, \omega)$ (Appendix A). This kind of resonance is called additional resonance, because it is not present in the Orr-Ward formula. When Γ_1 is rather small compared with Γ_2 , the intensities of some additional peaks can be much larger than those of two-photon resonances. This is clearly demonstrated by Fig. 3(c), where reducing Γ_1 to the value of $0.001t$ results in a drastic increase of the additional peak, which considerably exceeds the unchanged two-photon resonance peaks. Moreover, at a photon energy near $0.5t$ a negative resonant peak is observed, which certainly cannot be assigned to a two-photon resonance. Indeed, experiments have shown that in conjugated polymers Γ_1^{-1} is typically 1–3 ps,²⁰ whereas Γ_2^{-1} is less than 50 fs,²¹ implying that Γ_1 is an order of magnitude smaller than Γ_2 .

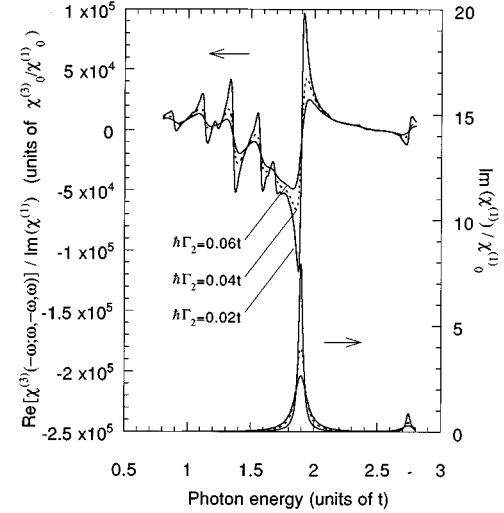


FIG. 4. The spectra of the figure of merit and linear absorption for the polymer ring of $N=20$ sites with $\delta t = 0.2t$, $\hbar\Gamma_1 = 0.001t$, and various Γ_2 .

Therefore one has to be careful in interpreting experimental data of two-photon absorption.

To understand Figs. 3(b) and 3(c), one should analyze the contribution of the first and third terms from blocks (A3), (A4), (A6), and (A7) in the expression of $\chi^{(3)}(-\omega; \omega, -\omega, \omega)$ (Appendix A),

$$\begin{aligned}
& +2 \sum_{l,m,n} \frac{\langle g|P|n\rangle\langle n|P|m\rangle\langle m|P|l\rangle\langle l|P|g\rangle}{(\omega + \omega_{nm} + i\Gamma_{mn})(\omega_{nl} + i\Gamma_{ln})(gq - \omega_{lg} + i\Gamma_{lg})} + 2 \sum_{l,m,n} \frac{\langle g|P|n\rangle\langle n|P|m\rangle\langle m|P|l\rangle\langle l|P|g\rangle}{(\omega + \omega_{nm} + i\Gamma_{mn})(\omega_{nl} + i\Gamma_{ln})(-\omega - \omega_{lg} + i\Gamma_{lg})} \\
& + 2 \sum_{l,m,n} \frac{\langle g|P|n\rangle\langle n|P|m\rangle\langle m|P|l\rangle\langle l|P|g\rangle}{(\omega + \omega_{nm} + i\Gamma_{mn})(\omega_{nl} + i\Gamma_{ln})(\omega + \omega_{ng} + i\Gamma_{gn})} + 2 \sum_{l,m,n} \frac{\langle g|P|n\rangle\langle n|P|m\rangle\langle m|P|l\rangle\langle l|P|g\rangle}{(\omega + \omega_{nm} + i\Gamma_{mn})(\omega_{nl} + i\Gamma_{ln})(-\omega + \omega_{ng} + i\Gamma_{gn})} \\
& - 2 \sum_{l,m,n} \frac{\langle g|P|n\rangle\langle n|P|m\rangle\langle m|P|l\rangle\langle l|P|g\rangle}{(\omega + \omega_{ml} + i\Gamma_{lm})(\omega_{nl} + i\Gamma_{ln})(\omega + \omega_{ng} + i\Gamma_{gn})} - 2 \sum_{l,m,n} \frac{\langle g|P|n\rangle\langle n|P|m\rangle\langle m|P|l\rangle\langle l|P|g\rangle}{(\omega + \omega_{ml} + i\Gamma_{lm})(\omega_{nl} + i\Gamma_{ln})(-\omega + \omega_{ng} + i\Gamma_{gn})} \\
& - 2 \sum_{l,m,n} \frac{\langle g|P|n\rangle\langle n|P|m\rangle\langle m|P|l\rangle\langle l|P|g\rangle}{(\omega + \omega_{ml} + i\Gamma_{lm})(\omega_{nl} + i\Gamma_{ln})(\omega - \omega_{lg} + i\Gamma_{lg})} - 2 \sum_{l,m,n} \frac{\langle g|P|n\rangle\langle n|P|m\rangle\langle m|P|l\rangle\langle l|P|g\rangle}{(\omega + \omega_{ml} + i\Gamma_{lm})(\omega_{nl} + i\Gamma_{ln})(-\omega - \omega_{lg} + i\Gamma_{lg})}, \quad (4)
\end{aligned}$$

where n and l label one-photon excited states, m numerates two-photon excited states, g means the ground state, and $\omega_{ij} = (E_i - E_j)/\hbar$. This can be reduced to

$$\begin{aligned}
& 2 \sum_{l,m,n} \langle g|P|n\rangle\langle n|P|m\rangle\langle m|P|l\rangle\langle l|P|g\rangle \left[\frac{1}{(\omega + \omega_{ng} + i\Gamma_{gn})(-\omega - \omega_{lg} + i\Gamma_{lg})} + \frac{1}{(-\omega + \omega_{ng} + i\Gamma_{gn})(\omega - \omega_{lg} + i\Gamma_{lg})} \right] \\
& \times \frac{[\omega_{ng} - \omega_{lg} + i(\Gamma_{lg} + \Gamma_{gn})][\omega_{nl} - 2\omega_{nm} + i(\Gamma_{lm} - \Gamma_{mn})]}{(\omega_{nl} + i\Gamma_{ln})(\omega + \omega_{nm} + i\Gamma_{mn})(\omega + \omega_{ml} + i\Gamma_{lm})}. \quad (5)
\end{aligned}$$

The additional resonances come from the terms with $n=l$, in which the last multiple is

$$- \frac{4\Gamma_2}{\Gamma_1} \frac{\omega_{nm}}{(\omega + \omega_{nm} + i\Gamma_2)(\omega - \omega_{nm} + i\Gamma_2)}, \quad (6)$$

where we assume all transverse damping constants to be the same and equal to Γ_2 . It is apparent that additional resonances can be both positive and negative depending on the sign of ω_{nm} . The Γ_1^{-1} dependence is easy to see if one compares Figs. 3(b) and 3(c).

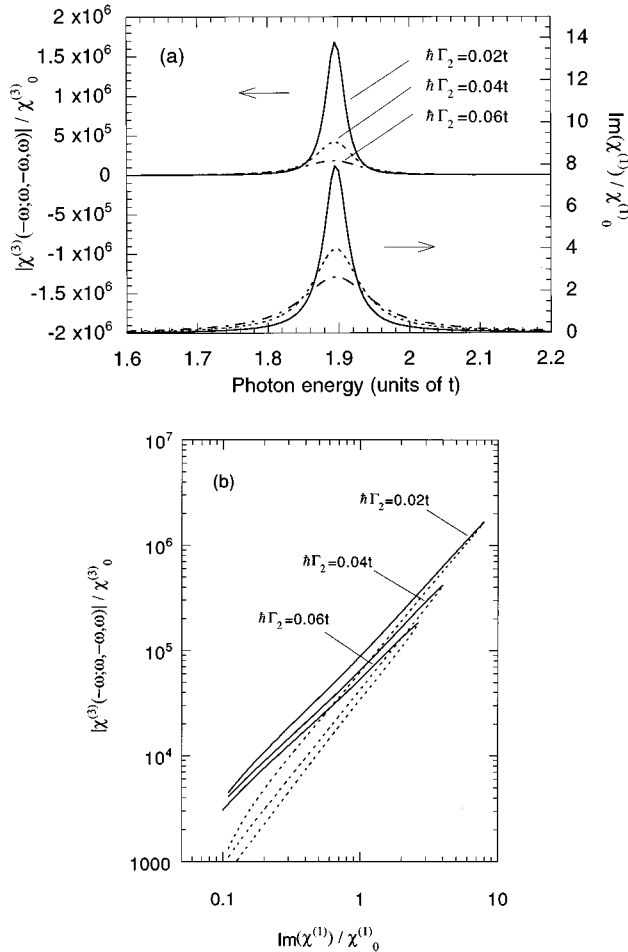


FIG. 5. (a) The absolute value of $\chi^{(3)}(-\omega; \omega, -\omega, \omega)$ and the imaginary part of $\chi^{(1)}(\omega)$ as functions of photon energy in the region of the lowest one-photon resonance for the polymer ring of $N=20$ sites with $\delta t=0.02t$, $\hbar\Gamma_1=0.001t$, and various Γ_2 . (b) The absolute value of $\chi^{(3)}(-\omega; \omega, -\omega, \omega)$ as a function of the imaginary part of $\chi^{(1)}(\omega)$. The solid lines correspond to the low-energy side of the resonance peak and the dashed lines correspond to the high-energy side.

The existence of extra resonances was discussed in the past in a different context. Bloembergen, Lotem, and Lynch¹³ pointed out the presence of dephasing-induced Raman-type extra resonances in the general expression of four-wave mixing, $\chi^{(3)}(-\omega_p; \omega_1, -\omega_2, \omega_3)$. The effect was later observed in Na vapor as a pressure-induced resonance.¹⁴ This type of extra resonance occurs when the *frequency difference* $\omega_1 - \omega_2$ or $\omega_3 - \omega_1$ corresponds to an energy difference between two initially unpopulated excited states. Obviously it is different from the one discussed here for degenerate four-wave mixing, where the extra resonance condition is that the frequency ω itself corresponds to an energy difference between excited states. Furthermore, the Γ_1^{-1} dependence in expression (6) is specific to the present case, and is absent in the Raman-type resonance. To our best knowledge there have been no experimental studies of the type or extra resonances discussed here.

A figure of merit is always a matter of interest in searching for nonlinear optical materials. In Fig. 4 we present the ω dependence of the ratio $\text{Re}[\chi^{(3)}(-\omega; \omega, -\omega, \omega)]/\text{Im}[\chi^{(1)}(\omega)]$ for various Γ_2 , together with the linear absorption

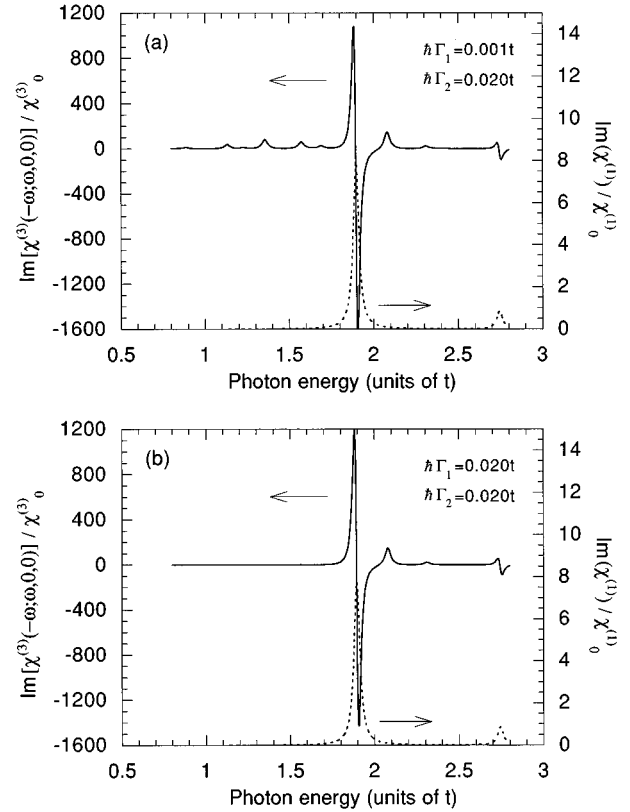


FIG. 6. The spectra of the electroabsorption (solid line) and linear absorption (dashed line) for the polymer ring of $N=20$ sites with $\delta t=0.2t$ and $\hbar\Gamma_2=0.020t$. (a) $\hbar\Gamma_1=0.001t$. (b) $\hbar\Gamma_1=0.020t$.

$\text{Im}[\chi^{(1)}(\omega)]$. It is easy to see that the ratio has a considerable magnitude in the relatively wide spectral region (usually, t is about 2 eV) just below the one-photon resonance. Such a wide region adds another attractive feature to conjugated polymers as promising candidates for future applications.

Another interesting issue related to the figure of merit is a so-called scaling law¹⁵—a relationship between $|\chi^{(3)}(-\omega; \omega, -\omega, \omega)|$ and $\text{Im}[\chi^{(1)}(\omega)]$. Examples of the two quantities are plotted in Fig. 5(a) as functions of ω for various Γ_2 . The dependence of $|\chi^{(3)}(-\omega; \omega, -\omega, \omega)|$ upon $\text{Im}[\chi^{(1)}(\omega)]$ is presented in Fig. 5(b). The solid lines correspond to the low-energy side of the linear absorption peak, and the dashed ones to the high-energy side. As a whole these lines indicate a power-law behavior

$$|\chi^{(3)}(-\omega; \omega, -\omega, \omega)| \approx c \{ \text{Im}[\chi^{(1)}(\omega)] \}^p. \quad (7)$$

The exponent p is close to 1 ($p \sim 1.2$) on the low-energy side, while it is much larger than 1 ($p \sim 1.7$) on the high-energy side. What should be noted here is that the coefficient c rapidly decreases upon increasing the transverse damping constant Γ_2 . Due to the relative simplicity of measuring the absolute value of $\chi^{(3)}(-\omega; \omega, -\omega, \omega)$, this fact can be useful for an estimation of Γ_2 .

IV. ELECTROABSORPTION

The electromodulation spectrum $\chi^{(3)}(-\omega; \omega, 0, 0)$ obtained in the density-matrix formalism also demonstrates some specific features, which are lost in the Orr-Ward approach. Fig-

ure 6(a) presents the electroabsorption spectrum together with the linear absorption for a polymer ring with $N=20$ sites and damping constants $\hbar\Gamma_1=0.001t$ and $\hbar\Gamma_2=0.02t$. What we want to pay attention to at this stage is a group of small peaks in the photon energy region below the one-photon resonance. They are the same sort of additional reso-

nances as seen in the two-photon absorption spectra of Fig. 3, each resonance corresponding to an energy difference between excited levels. To make it clear, we consider the sum of the last terms in the four blocks (B3), (B4), (B6), and (B7) of the expression for $\chi^{(3)}(-\omega;\omega,0,0)$ presented in Appendix B:

$$+2 \sum_{l,m,n} \frac{\langle g|P|n\rangle\langle n|P|m\rangle\langle m|P|l\rangle\langle l|P|g\rangle}{(\omega + \omega_{nm} + i\Gamma_{mn})(\omega_{nl} + i\Gamma_{ln})(-\omega_{lg} + i\Gamma_{lg})} + 2 \sum_{l,m,n} \frac{\langle g|P|n\rangle\langle n|P|m\rangle\langle m|P|l\rangle\langle l|P|g\rangle}{(\omega + \omega_{nm} + i\Gamma_{mn})(\omega_{nl} + i\Gamma_{ln})(\omega_{ng} + i\Gamma_{gn})} \\ - 2 \sum_{l,m,n} \frac{\langle g|P|n\rangle\langle n|P|m\rangle\langle m|P|l\rangle\langle l|P|g\rangle}{(\omega + \omega_{ml} + i\Gamma_{lm})(\omega_{nl} + i\Gamma_{ln})(\omega_{ng} + i\Gamma_{gn})} - 2 \sum_{l,m,n} \frac{\langle g|P|n\rangle\langle n|P|m\rangle\langle m|P|l\rangle\langle l|P|g\rangle}{(\omega + \omega_{ml} + i\Gamma_{lm})(\omega_{nl} + i\Gamma_{ln})(-\omega_{lg} + i\Gamma_{lg})}. \quad (8)$$

This can be reduced to

$$+ 2 \sum_{l,m,n} \frac{\langle g|P|n\rangle\langle n|P|m\rangle\langle m|P|l\rangle\langle l|P|g\rangle}{(\omega_{ng} + i\Gamma_{gn})(-\omega_{lg} + i\Gamma_{lg})} \frac{[\omega_{ng} - \omega_{lg} + i(\Gamma_{gn} + \Gamma_{lg})][\omega_{nl} - 2\omega_{nm} + i(\Gamma_{lm} - \Gamma_{mn})]}{(\omega_{nl} + i\Gamma_{ln})(\omega + \omega_{nm} + i\Gamma_{mn})(\omega + \omega_{ml} + i\Gamma_{lm})}. \quad (9)$$

The resonances come from the terms with $l=n$, the contribution of which, using notations Γ_1 and Γ_2 , can be represented as

$$- \frac{8\Gamma_2}{\Gamma_1} \sum_{m,n} \frac{|\langle g|P|n\rangle|^2 |\langle n|P|m\rangle|^2}{(\omega_{ng} + i\Gamma_2)(-\omega_{ng} + i\Gamma_2)} \\ \times \frac{\omega_{nm}}{(\omega + \omega_{nm} + i\Gamma_2)(\omega - \omega_{nm} + i\Gamma_2)}. \quad (10)$$

The peaks corresponding to the additional resonances can be observed only when Γ_1 is small enough. Similar to the case of two-photon absorption, in which the intensity of additional resonance peaks is drastically reduced when Γ_1 is increased, the same effect occurs for the corresponding resonances in the electroabsorption spectrum as well. Figure 6(b) shows the electroabsorption spectrum calculated with only one parameter Γ_1 , changed referring to the case presented in Fig. 6(a). In Fig. 6(b), $\hbar\Gamma_1 = \hbar\Gamma_2 = 0.02t$, and small peaks below the one-photon resonance are so strongly decreased due to large Γ_1 that they just cannot be seen.

An analysis of both the expression for $\chi^{(3)}(-\omega;\omega,0,0)$ and calculated spectra shows that forbidden transitions to two-photon excited states [more specifically, A^- ($|K|=0,2$) states; see Ref. 10] practically do not reveal themselves as strong peaks in the electroabsorption spectra. The reason is that allowed one-photon transitions and additional resonances discussed here contribute to $\chi^{(3)}(-\omega;\omega,0,0)$ through the terms proportional to Γ_2^{-2} (the first term in the expression of Appendix A) and Γ_1^{-1} , respectively, while the forbidden transitions only through Γ_2^{-1} . An observation of the additional resonances can be assured by taking a very small Γ_1 , but a signal due to a forbidden transition is always much smaller than that due to an allowed one. It should be noted here that such a conclusion is valid only until an applied static electric field becomes very large and makes a perturbation solution inapplicable.

As already mentioned, a direct measurement of transverse relaxation time in conjugated polymers is a challenging subject for experimentalists because of a large inhomogeneous broadening existing in actual systems. Various indirect methods can facilitate an evaluation of such an important parameter. That is why here we have analyzed the evolution of the electroabsorption spectrum with varying Γ_2 . Since the intensity of the electroabsorption spectrum in the region of the one-photon resonance is proportional to Γ_2^{-2} , a signal here is expected to be rather sensitive to the magnitude of the transverse damping constant. Figures 6(a) and 7, which correspond to $\hbar\Gamma_2$ increasing from $0.02t$ [Fig. 6(b)] to $0.10t$, clearly corroborate such an assumption. A very intense positive peak just below the lowest one-photon resonance [Fig. 6(a)] practically disappears after an increase of $\hbar\Gamma_2$ from $0.02t$ till $0.06t$. This peak can be a good indicator for a magnitude of the transverse broadening.

The extra resonance discussed here is an effect of damping in $\chi^{(3)}$ processes. There is a completely different method

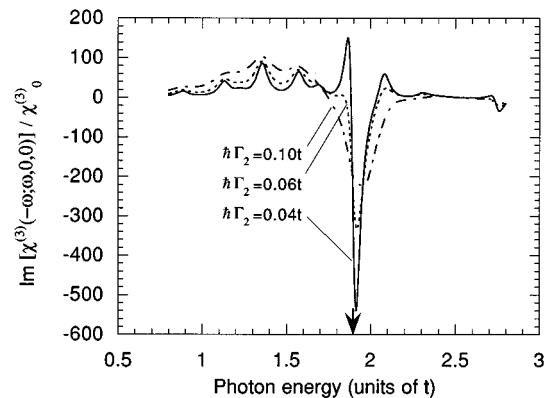


FIG. 7. The electroabsorption spectra for the polymer ring of $N=20$ sites with $\delta t=0.2t$, $\hbar\Gamma_1=0.001t$, and various Γ_2 . The vertical arrow points the lowest one-photon resonance.

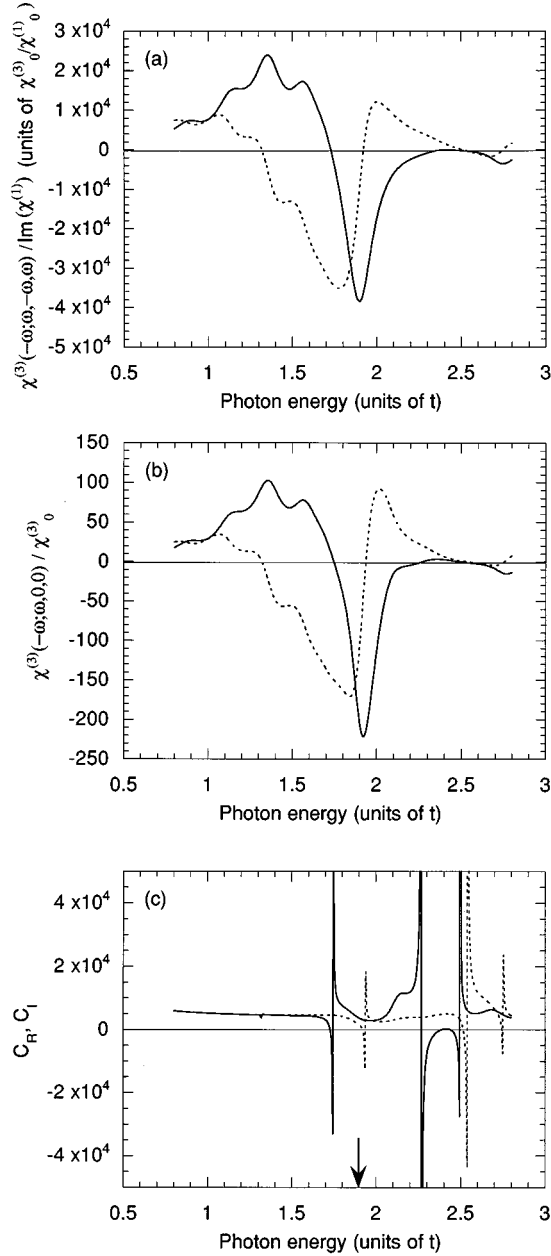


FIG. 8. (a) The real (dashed line) and imaginary (solid line) parts of $\chi^{(3)}(-\omega; \omega, -\omega, \omega)$ divided by $\text{Im}[\chi^{(1)}]$ as functions of photon energy for the polymer ring of $N=20$ sites with $\delta t=0.2t$, $\hbar\Gamma_1=0.001t$, and $\hbar\Gamma_2=0.100t$. (b) The real (dashed line) and imaginary (solid line) parts of $\chi^{(3)}(-\omega; \omega, 0, 0)$ as functions of photon energy for the same polymer ring. (c) The ratios of (a) plots over corresponding (b) plots multiplied by N ; that is, the proportionality factors C_R and C_I . The vertical arrow points the lowest one-photon resonance.

of calculating electroabsorption without using the $\chi^{(3)}$ formula—by calculating linear absorption spectra with and without a finite electric field and by taking the difference between them.²² This approach does not give any extra resonance, because it can take damping into account only in linear absorption processes. Which of the two approaches is a better description of real experiments may depend on the strength of the electric field and the magnitude of the damping.

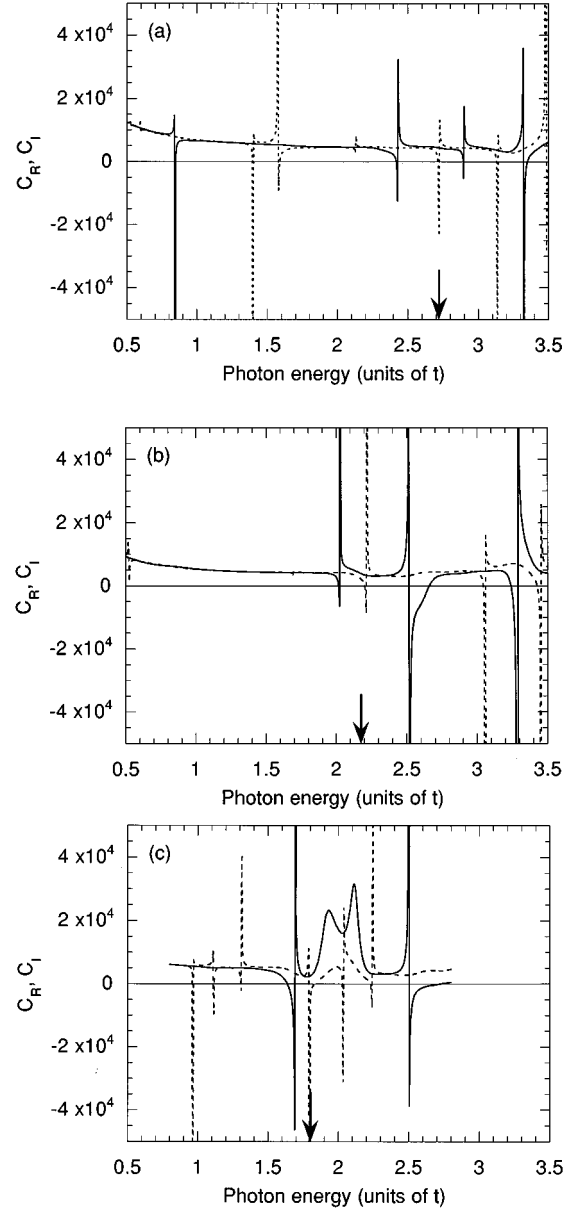


FIG. 9. The proportionality factors C_R (dashed line) and C_I (solid line) as functions of photon energy for the polymer rings with $\delta t=0.2t$, $\hbar\Gamma_1=0.001t$, $\hbar\Gamma_2=0.100t$, and various number of sites, N . (a) $N=6$. (b) $N=12$. (c) $N=22$.

V. RELATIONSHIP BETWEEN $\chi^{(3)}(-\omega; \omega, -\omega, \omega)$ AND $\chi^{(3)}(-\omega; \omega, 0, 0)$

There is one more interesting feature of $\chi^{(3)}(-\omega; \omega, -\omega, \omega)$ and $\chi^{(3)}(-\omega; \omega, 0, 0)$ spectra that is worth mentioning. In cases when the transverse damping constant is about two orders of magnitude larger than the longitudinal one, we numerically observe the relations

$$N \text{Re}[\chi^{(3)}(-\omega; \omega, -\omega, \omega)]\chi_0^{(1)} \approx C_R \text{Re}[\chi^{(3)}(-\omega; \omega, 0, 0)]\text{Im}[\chi^{(1)}(\omega)], \quad (11a)$$

$$N \text{Im}[\chi^{(3)}(-\omega; \omega, -\omega, \omega)]\chi_0^{(1)} \approx C_I \text{Im}[\chi^{(3)}(-\omega; \omega, 0, 0)]\text{Im}[\chi^{(1)}(\omega)], \quad (11b)$$

where all susceptibilities are those per site, and the proportionality factors C_R and C_I are practically equal and do not depend upon N and ω in a very wide range of photon energies. In other words, we can write an approximate equality

$$N\chi^{(3)}(-\omega; \omega, -\omega, \omega)\chi_0^{(1)} \approx C\chi^{(3)}(-\omega; \omega, 0, 0) \times \text{Im}[\chi^{(1)}(\omega)], \quad (12)$$

with a real factor C independent of N and ω . This relation can help in the evaluation of $\chi^{(3)}(-\omega; \omega, -\omega, \omega)$ for materials with $\Gamma_2 \gg \Gamma_1$ on the basis of linear and electromodulation spectra, which are relatively easier to measure.

To become convinced of this, one should look at Fig. 8. Figure 8(a) shows real and imaginary parts of $\chi^{(3)}(-\omega; \omega, -\omega, \omega)$ divided by $\text{Im}[\chi^{(1)}(\omega)]$ for a polymer ring with $N=20$ sites, $\hbar\Gamma_1=0.001t$ and $\hbar\Gamma_2=0.100t$. Figure 8(b) gives $\chi^{(3)}(-\omega; \omega, 0, 0)$ for the same polymer ring. Obviously, these two figures are very alike. Figure 8(c) shows ratios of (a) plots over corresponding (b) plots multiplied by N , i.e., the factors C_R and C_I . Up and down leaps of the plots in Fig. 8(c) take place for photon energies at which the corresponding plots in Fig. 8(a) and 8(b) cross a zero line, and since they cross it at slightly different photon energies the leaps occur. Setting aside these leaps we can conclude that, as a whole; C_R and C_I coincide and do not change with photon energy. This is especially true for the spectral region of two-photon absorption below $1.9t$. To show the independence of C_R and C_I from N , here we present their spectra for rings with $N=6, 12$, and 22 sites [Figs. 9(a), 9(b), and 9(c), respectively], all other parameters being the same as in Fig. 8(c). Again ignoring the leaps we can see that all plots are at the same level, about 5×10^3 . For relatively large $N=22$ [Fig. 9(c)] there is rather a wide region just above one-photon resonance (shown by vertical arrow), where a deviation from that level does not look like a sharp splash, but for the range of two-photon absorption all the features are still satisfactory. Unfortunately, an analytical derivation of relation (11) seems to be too cumbersome for such a wide spectral region; therefore in this work we have restricted ourselves to a numerical consideration.

VI. CONCLUSIONS

We have studied the $\chi^{(3)}$ spectrum of conjugated polymers within the Pariser-Parr-Pople model. Several interesting aspects of $\chi^{(3)}$ have been elucidated. First of all, the linear relationship between the magnitude of $\chi^{(3)}(-\omega; \omega, -\omega, \omega)$ for degenerate four-wave mixing and the linear absorption spectrum $\alpha(\omega)$ approximately holds on the low-energy side of the exciton peak, when the transverse relaxation rate Γ_2 is much larger than the longitudinal relaxation rate Γ_1 . The linearity coefficient $\chi^{(3)}/\alpha$ is strongly dependent on Γ_2 , and approximately inversely proportional to Γ_2 . Under the same condition $\Gamma_2 \gg \Gamma_1$, additional peaks due to extra resonances among excited states appear, and can be much larger than the ordinary two-photon absorption peaks. This implies that we have to be very careful about the interpretation of observed $\chi^{(3)}$ spectra as two-photon absorption. Similar additional resonances show up in the electromodulation spectrum $\chi^{(3)}(-\omega; \omega, 0, 0)$. Finally we have shown numerically an approximate relationship $\chi^{(3)}(-\omega; \omega, -\omega, \omega) \approx \alpha(\omega)\chi^{(3)}(-\omega; \omega, 0, 0)$. All these features are dependent on the ratio Γ_2/Γ_1 , hence a systematic experimental investigation of $\chi^{(3)}$ spectra with a determination of the relevant relaxation rates would be strongly desirable.

ACKNOWLEDGMENTS

The authors wish to thank E. Hanamura and J. Inoue for stimulating conversations. One of the authors (S.A.) thanks A. Esser, M. Schreiber, and C. Bubeck for useful discussions.

APPENDIX A

The third-order nonlinear optical susceptibility $\chi^{(3)}(-\omega; \omega, -\omega, \omega)$ per site of an N -site molecule is written with the dipole operator P as follows:

$$\begin{aligned} \chi^{(3)}(-\omega; \omega, -\omega, \omega) = & \frac{1}{6N\hbar^3} \left\{ -2 \sum_{l,m,n} \frac{\langle g|P|n\rangle\langle n|P|m\rangle\langle m|P|l\rangle\langle l|P|g\rangle}{(\omega - \omega_{ng} + i\Gamma_{ng})(-\omega_{mg} + i\Gamma_{mg})(\omega - \omega_{lg} + i\Gamma_{lg})} \right. \\ & -2 \sum_{l,m,n} \frac{\langle g|P|n\rangle\langle n|P|m\rangle\langle m|P|l\rangle\langle l|P|g\rangle}{(\omega - \omega_{ng} + i\Gamma_{ng})(2\omega - \omega_{mg} + i\Gamma_{mg})(\omega - \omega_{lg} + i\Gamma_{lg})} \\ & -2 \sum_{l,m,n} \frac{\langle g|P|n\rangle\langle n|P|m\rangle\langle m|P|l\rangle\langle l|P|g\rangle}{(\omega - \omega_{ng} + i\Gamma_{ng})(-\omega_{mg} + i\Gamma_{mg})(-\omega - \omega_{lg} + i\Gamma_{lg})} \\ & +2 \sum_{l,m,n} \frac{\langle g|P|n\rangle\langle n|P|m\rangle\langle m|P|l\rangle\langle l|P|g\rangle}{(\omega + \omega_{nm} + i\Gamma_{mn})(-\omega_{mg} + i\Gamma_{mg})(\omega - \omega_{lg} + i\Gamma_{lg})} \\ & +2 \sum_{l,m,n} \frac{\langle g|P|n\rangle\langle n|P|m\rangle\langle m|P|l\rangle\langle l|P|g\rangle}{(\omega + \omega_{nm} + i\Gamma_{mn})(2\omega - \omega_{mg} + i\Gamma_{mg})(\omega - \omega_{lg} + i\Gamma_{lg})} \\ & \left. +2 \sum_{l,m,n} \frac{\langle g|P|n\rangle\langle n|P|m\rangle\langle m|P|l\rangle\langle l|P|g\rangle}{(\omega + \omega_{nm} + i\Gamma_{mn})(-\omega_{mg} + i\Gamma_{mg})(-\omega - \omega_{lg} + i\Gamma_{lg})} \right\} \quad (A1) \end{aligned}$$

$$\begin{aligned} & +2 \sum_{l,m,n} \frac{\langle g|P|n\rangle\langle n|P|m\rangle\langle m|P|l\rangle\langle l|P|g\rangle}{(\omega + \omega_{nm} + i\Gamma_{mn})(-\omega_{mg} + i\Gamma_{mg})(\omega - \omega_{lg} + i\Gamma_{lg})} \\ & +2 \sum_{l,m,n} \frac{\langle g|P|n\rangle\langle n|P|m\rangle\langle m|P|l\rangle\langle l|P|g\rangle}{(\omega + \omega_{nm} + i\Gamma_{mn})(2\omega - \omega_{mg} + i\Gamma_{mg})(\omega - \omega_{lg} + i\Gamma_{lg})} \\ & +2 \sum_{l,m,n} \frac{\langle g|P|n\rangle\langle n|P|m\rangle\langle m|P|l\rangle\langle l|P|g\rangle}{(\omega + \omega_{nm} + i\Gamma_{mn})(-\omega_{mg} + i\Gamma_{mg})(-\omega - \omega_{lg} + i\Gamma_{lg})} \quad (A2) \end{aligned}$$

APPENDIX B

The third-order nonlinear optical susceptibility $\chi^{(3)}(-\omega; \omega, 0, 0)$ per site of an N -site molecule at zero temperature is written as follows:

$$\begin{aligned} \chi^{(3)}(-\omega; \omega, 0, 0) = & \frac{1}{6N\hbar^3} \left\{ -2 \sum_{l,m,n} \frac{\langle g|P|n\rangle \langle n|P|m\rangle \langle m|P|l\rangle \langle l|P|g\rangle}{(\omega - \omega_{ng} + i\Gamma_{ng})(\omega - \omega_{mg} + i\Gamma_{mg})(\omega - \omega_{lg} + i\Gamma_{lg})} \right. \\ & -2 \sum_{l,m,n} \frac{\langle g|P|n\rangle \langle n|P|m\rangle \langle m|P|l\rangle \langle l|P|g\rangle}{(\omega - \omega_{ng} + i\Gamma_{ng})(\omega - \omega_{mg} + i\Gamma_{mg})(-\omega_{lg} + i\Gamma_{lg})} \\ & -2 \sum_{l,m,n} \frac{\langle g|P|n\rangle \langle n|P|m\rangle \langle m|P|l\rangle \langle l|P|g\rangle}{(\omega - \omega_{ng} + i\Gamma_{ng})(-\omega_{mg} + i\Gamma_{mg})(-\omega_{lg} + i\Gamma_{lg})} \end{aligned} \quad (B1)$$

$$\begin{aligned} & +2 \sum_{l,m,n} \frac{\langle g|P|n\rangle \langle n|P|m\rangle \langle m|P|l\rangle \langle l|P|g\rangle}{(\omega + \omega_{nm} + i\Gamma_{mn})(\omega - \omega_{mg} + i\Gamma_{mg})(\omega - \omega_{lg} + i\Gamma_{lg})} \\ & +2 \sum_{l,m,n} \frac{\langle g|P|n\rangle \langle n|P|m\rangle \langle m|P|l\rangle \langle l|P|g\rangle}{(\omega + \omega_{nm} + i\Gamma_{mn})(\omega - \omega_{mg} + i\Gamma_{mg})(-\omega_{lg} + i\Gamma_{lg})} \\ & +2 \sum_{l,m,n} \frac{\langle g|P|n\rangle \langle n|P|m\rangle \langle m|P|l\rangle \langle l|P|g\rangle}{(\omega + \omega_{nm} + i\Gamma_{mn})(-\omega_{mg} + i\Gamma_{mg})(-\omega_{lg} + i\Gamma_{lg})} \end{aligned} \quad (B2)$$

$$\begin{aligned} & +2 \sum_{l,m,n} \frac{\langle g|P|n\rangle \langle n|P|m\rangle \langle m|P|l\rangle \langle l|P|g\rangle}{(\omega + \omega_{nm} + i\Gamma_{mn})(\omega + \omega_{nl} + i\Gamma_{ln})(\omega - \omega_{lg} + i\Gamma_{lg})} \\ & +2 \sum_{l,m,n} \frac{\langle g|P|n\rangle \langle n|P|m\rangle \langle m|P|l\rangle \langle l|P|g\rangle}{(\omega + \omega_{nm} + i\Gamma_{mn})(\omega + \omega_{nl} + i\Gamma_{ln})(-\omega_{lg} + i\Gamma_{lg})} \\ & +2 \sum_{l,m,n} \frac{\langle g|P|n\rangle \langle n|P|m\rangle \langle m|P|l\rangle \langle l|P|g\rangle}{(\omega + \omega_{nm} + i\Gamma_{mn})(\omega_{nl} + i\Gamma_{ln})(-\omega_{lg} + i\Gamma_{lg})} \end{aligned} \quad (B3)$$

$$\begin{aligned} & +2 \sum_{l,m,n} \frac{\langle g|P|n\rangle \langle n|P|m\rangle \langle m|P|l\rangle \langle l|P|g\rangle}{(\omega + \omega_{nm} + i\Gamma_{mn})(\omega + \omega_{nl} + i\Gamma_{ln})(\omega + \omega_{ng} + i\Gamma_{gn})} \\ & +2 \sum_{l,m,n} \frac{\langle g|P|n\rangle \langle n|P|m\rangle \langle m|P|l\rangle \langle l|P|g\rangle}{(\omega + \omega_{nm} + i\Gamma_{mn})(\omega + \omega_{nl} + i\Gamma_{ln})(\omega_{ng} + i\Gamma_{gn})} \\ & +2 \sum_{l,m,n} \frac{\langle g|P|n\rangle \langle n|P|m\rangle \langle m|P|l\rangle \langle l|P|g\rangle}{(\omega + \omega_{nm} + i\Gamma_{mn})(\omega_{nl} + i\Gamma_{ln})(\omega_{ng} + i\Gamma_{gn})} \end{aligned} \quad (B4)$$

$$\begin{aligned} & -2 \sum_{l,m,n} \frac{\langle g|P|n\rangle \langle n|P|m\rangle \langle m|P|l\rangle \langle l|P|g\rangle}{(\omega + \omega_{ml} + i\Gamma_{lm})(\omega + \omega_{mg} + i\Gamma_{gm})(\omega + \omega_{ng} + i\Gamma_{gn})} \\ & -2 \sum_{l,m,n} \frac{\langle g|P|n\rangle \langle n|P|m\rangle \langle m|P|l\rangle \langle l|P|g\rangle}{(\omega + \omega_{ml} + i\Gamma_{lm})(\omega + \omega_{mg} + i\Gamma_{gm})(\omega_{ng} + i\Gamma_{gn})} \\ & -2 \sum_{l,m,n} \frac{\langle g|P|n\rangle \langle n|P|m\rangle \langle m|P|l\rangle \langle l|P|g\rangle}{(\omega + \omega_{ml} + i\Gamma_{lm})(\omega_{mg} + i\Gamma_{gm})(\omega_{ng} + i\Gamma_{gn})} \end{aligned} \quad (B5)$$

$$\begin{aligned} & -2 \sum_{l,m,n} \frac{\langle g|P|n\rangle \langle n|P|m\rangle \langle m|P|l\rangle \langle l|P|g\rangle}{(\omega + \omega_{ml} + i\Gamma_{lm})(\omega + \omega_{nl} + i\Gamma_{ln})(\omega + \omega_{ng} + i\Gamma_{gn})} \\ & -2 \sum_{l,m,n} \frac{\langle g|P|n\rangle \langle n|P|m\rangle \langle m|P|l\rangle \langle l|P|g\rangle}{(\omega + \omega_{ml} + i\Gamma_{lm})(\omega + \omega_{nl} + i\Gamma_{ln})(\omega_{ng} + i\Gamma_{gn})} \\ & -2 \sum_{l,m,n} \frac{\langle g|P|n\rangle \langle n|P|m\rangle \langle m|P|l\rangle \langle l|P|g\rangle}{(\omega + \omega_{ml} + i\Gamma_{lm})(\omega_{nl} + i\Gamma_{ln})(\omega_{ng} + i\Gamma_{gn})} \end{aligned} \quad (B6)$$

$$\begin{aligned}
& -2 \sum_{l,m,n} \frac{\langle g|P|n\rangle\langle n|P|m\rangle\langle m|P|l\rangle\langle l|P|g\rangle}{(\omega + \omega_{ml} + i\Gamma_{lm})(\omega + \omega_{nl} + i\Gamma_{ln})(\omega - \omega_{lg} + i\Gamma_{lg})} \\
& -2 \sum_{l,m,n} \frac{\langle g|P|n\rangle\langle n|P|m\rangle\langle m|P|l\rangle\langle l|P|g\rangle}{(\omega + \omega_{ml} + i\Gamma_{lm})(\omega + \omega_{nl} + i\Gamma_{ln})(-\omega_{lg} + i\Gamma_{lg})} \\
& -2 \sum_{l,m,n} \frac{\langle g|P|n\rangle\langle n|P|m\rangle\langle m|P|l\rangle\langle l|P|g\rangle}{(\omega + \omega_{ml} + i\Gamma_{lm})(\omega_{nl} + i\Gamma_{ln})(-\omega_{lg} + i\Gamma_{lg})} \tag{B7}
\end{aligned}$$

$$\begin{aligned}
& +2 \sum_{l,m,n} \frac{\langle g|P|n\rangle\langle n|P|m\rangle\langle m|P|l\rangle\langle l|P|g\rangle}{(\omega + \omega_{lg} + i\Gamma_{gl})(\omega + \omega_{mg} + i\Gamma_{gm})(\omega + \omega_{ng} + i\Gamma_{gn})} \\
& +2 \sum_{l,m,n} \frac{\langle g|P|n\rangle\langle n|P|m\rangle\langle m|P|l\rangle\langle l|P|g\rangle}{(\omega + \omega_{lg} + i\Gamma_{gl})(\omega + \omega_{mg} + i\Gamma_{gm})(\omega_{ng} + i\Gamma_{gn})} \\
& +2 \sum_{l,m,n} \frac{\langle g|P|n\rangle\langle n|P|m\rangle\langle m|P|l\rangle\langle l|P|g\rangle}{(\omega + \omega_{lg} + i\Gamma_{gl})(\omega_{mg} + i\Gamma_{gm})(\omega_{ng} + i\Gamma_{gn})}. \tag{B8}
\end{aligned}$$

*Present address: Electrotechnical Laboratory, 1-1-4 Umezono, Tsukuba 305, Japan.

¹C. Sauteret, J. P. Hermann, R. Frey, F. Pradere, J. Ducuing, R. H. Baughman, and R. R. Chance, *Phys. Rev. Lett.* **36**, 956 (1976).

²G. M. Carter, M. K. Thakur, Y. J. Chen, and J. V. Hryniewicz, *Appl. Phys.* **47**, 457 (1985).

³S. Etemad and Z. G. Soos, in *Spectroscopy of Advanced Materials*, edited by R. J. H. Clark and R. E. Hester (Wiley, Chichester, 1991), Chap. 2.

⁴B. I. Greene, J. Orenstein, and S. Schmitt-Rink, *Science* **247**, 679 (1990).

⁵T. Kanetake, K. Ishikawa, T. Hasegawa, T. Koda, K. Takeda, M. Hasegawa, K. Kubodera, and H. Kobayashi, *Appl. Phys. Lett.* **54**, 2287 (1989).

⁶S. Abe, M. Schreiber, W. P. Su, and J. Yu, *Phys. Rev. B* **45**, 9432 (1992).

⁷S. Abe, in *Relaxation in Polymers*, edited by T. Kobayashi (World Scientific, Singapore, 1993), p. 215.

⁸D. Guo, S. Mazumdar, S. N. Dixit, F. Kajzar, F. Jarka, Y. Kawabe, and N. Peyghambarian, *Phys. Rev. B* **48**, 1433 (1993).

⁹V. A. Shakin and S. Abe, *Mol. Cryst. Liq. Cryst.* **256**, 643 (1994).

¹⁰V. A. Shakin and S. Abe, *Phys. Rev. B* **50**, 4306 (1994).

¹¹F. Guo, M. Chandross, and S. Mazumdar, *Phys. Rev. Lett.* **74**, 2086 (1995).

¹²B. J. Orr and J. F. Ward, *Mol. Phys.* **20**, 513 (1971).

¹³N. Bloembergen, H. Lotem, and R. T. Lynch, *Ind. J. Pure Appl. Phys.* **16**, 151 (1978).

¹⁴Y. Prior, A. R. Bogdan, M. Dagenais, and N. Bloembergen, *Phys. Rev. Lett.* **46**, 111 (1981).

¹⁵C. Bubeck, A. Kaltbeitzel, A. Grund, and M. LeClerc, *Chem. Phys.* **154**, 343 (1991).

¹⁶N. Bloembergen, *Nonlinear Optics* (Benjamin, New York, 1965).

¹⁷J.-L. Oudar and Y. R. Shen, *Phys. Rev. A* **22**, 1141 (1980).

¹⁸R. W. Boyd, *Nonlinear Optics* (Academic, London, 1992), Chap. 3.

¹⁹J. Inoue and E. Hanamura, *Nonlinear Opt.* **12**, 257 (1995).

²⁰T. Kobayashi, M. Yoshizawa, U. Stamm, M. Taiji, and M. Hasegawa, *J. Opt. Soc. Am.* **7**, 1558 (1990).

²¹T. Hattori and T. Kobayashi, *Chem. Phys. Lett.* **133**, 230 (1987).

²²Y. Kawabe, F. Jarka, N. Peyghambarian, D. Guo, S. Mazumdar, S. N. Dixit, and F. Kajzar, *Phys. Rev. B* **44**, 6530 (1991).